Kareem Mohammed Alnebhan, Muhaned A. Shallal

COMPOSITE CONCRETE AND CONCRETE FILLED STEEL TUBE (CFST) TRUSS GIRDERS

SPREGNUTE KONSTRUKCIJE OD BETONA I ČELIČNIH CEVI ISPUNJENIH BETONOM (CFST)

Originalni naučni rad / Original scientific paper
UDK /UDC:

Rad primljen / Paper received: 24.11.2019

Adresa autora / Author's address:
University of Al-Qadisiyah, Baghdad, Iraq
email: kmj72j@gmail.com

Keywords
- concrete-filled steel tube
- truss girders
- concrete deck slab
- shear connectors
- Warren truss
- composite concrete-steel

Ključne reči
- čelična cev ispunjena betonom
- rešetkasti nosači
- betonska podna ploča
- moždanici za spregnuti smičući spoj
- rešetka tipa Warren
- beton-čelik spregnuta konstrukcija

Abstract

The behaviour of concrete filled steel tube truss girders (CFST) with concrete deck slab is studied in this paper. The deflection, load capacity, failure modes and slip between the concrete slab and steel tube are reported. Eight specimens are tested under concentrated load at the mid-span, two of them without the concrete deck. The test parameters are: compressive strength (fcu) of concrete deck slab; fcu of concrete-filled steel tube for the lower chord; concrete slab's existence; location of concrete-filled tube and its existence; space between shear connectors and profile of the lower chord. Experimental results suggest that the concrete slab's existence, the strength of concrete slab, the steel section of bottom chord, and the strength of concrete that used to fill the bottom chord have a significant effect on the ultimate load, appearance of concrete slab cracks, deflection and slip. The space between shear connectors has a slight effect on the ultimate load and the deflection, but it has a great effect on the slip. Location of the concrete-filled tube has a significant effect on ultimate load and failure mode.

Izvod

U radu je proučeno ponašanje spojeva rešetkastih nosača od čeličnih cevi ispunjenih betonom (CFST) i betonskih podnih ploča. Razmotreni su: ugib, kapacitet opterećenja, tip loma i smicanje betonske ploče i čelične cevi. Ispitano je osam slučajeva sa koncentrisanim opterećenjem u sredini nosača, od kojih su dva bez betonske ploče. Parametri ispitivanja su: pritisna čvrstoća (fcu) betonske ploče; pritisna čvrstoća (fcu) čelične cevi ispunjene betonom u donjem pojasu; uticaj betonske ploče; uticaj i položaj cevi ispunjene betonom; rastojanje između moždanika spregnutog smičućeg spoja i profila donjeg pojasa. Eksperimentalni rezultati pokazuju da su uticaji: betonska ploča, čelični element donjeg pojasa i čvrstoća betona za punjenje donjeg pojasa - od značaja za: kapacitet opterećenja, pojavu prslina u betonskoj ploči, ugib i smicanje. Razmak moždanika ima mali uticaj na kapacitet opterećenja i ugib, ali ima veliki uticaj na smicanje. Položaj cevi ispunjene betonom ima veliki uticaj na kapacitet opterećenja i tip loma.

INTRODUCTION

The purpose of steel-concrete composite in structures is to keep the advantages of both materials: steel and concrete, /1/. The applications of composite beams can be found in many buildings and bridges, /2/. Concrete filled steel tubes (CFST) are widely used in civil engineering structures and propose many structural benefits. The CFST is used in columns /3/, beams /4-6/, and truss girders, /7/. The CFST enhances the tensile strength by about 11 % more than the hollow steel tube, /8/. Usually, CFT trusses contain concrete infilled chords and hollow braces. The CFST increases the compressive and tensile strength of the chords. It protects the steel tube of the upper chord from buckling inward and avoids pinching (inward contraction) of the steel tube of the lower chord. The CFST also increases the strength of the joints (brace to chord) and the whole flexural stiffness of the truss. The steel tube acts as a formwork for casting the concrete, /7, 9-11/.

Chan et al. /12/ studied two trusses, one with concrete filled truss members and the other with hollow truss members, experimentally and analytically. It turns out, when comparing the results, the load capacity of the truss with members filled with concrete is higher by 17.5 % than for the truss with hollow members. Huang et al. /13/ tested six specimens of different types of truss girders to study the effect of concrete-filled upper and lower chords of the truss with hollow chords on the welded joints. The author pointed out that concrete-filled upper and lower chords increased the strength and the rigidity of the joint, and evaded chord surface plastic failure. Warren-type truss girder has worked better than other types of truss girders and has a higher flexural rigidity and ultimate strength. In Xu et al. /14/ research, eight truss girders were tested (Warren truss), four curved CFST truss girders, two straight CFST truss girders, and two hollow chord curved truss girders. These specimens were employed to study their flexural behaviour, excluding the influence of the height-to-span ratio and the existence of concrete infill. The results revealed that the stiffness and the ultimate load of curved CFST truss girders are higher than for straight CFST truss girders and curved hollow truss girders. Chen et al. /15/ tested four kinds of

CFST trusses (multi-planar tubular), and reported the load capacity, deflection, the failure mode and strain intensity. The influences of upper and lower chords, diagonal and vertical braces, ductility and flexural rigidity of all specimens were also investigated. The failure modes, shown from the experimental work, consist of the surface plasticity, the local buckling, shear failure of the lower chord, the weld fracture and the end support failure. Fu et al. /16/ conducted one experimental test and numerical analysis to study the behaviour of spatial truss beam when lightweight aggregate concrete infilled steel tube (LACFST) is used. The performance was investigated by analysis of strains in the chords and webs, and the truss beam's deflection. Spatial truss beam (LACFST) failure occurred after excessive deflection, as the results revealed. The top chords failed under compressive yield, while the whole bottom chord section failed under tensile yield, at the mid-span. Huang et al. /17/ tested four experimental CFST truss specimens with various interfacial imperfections under four-point loading. They studied the influence of interfacial imperfections on the behaviour of CFST trusses. The result shows that the ultimate load is affected by interfacial imperfections between the concrete infill tube and steel tube, where the load capacity decreased when the depth separation of concrete increased. Zhou et al. /18/ tested four CFST trusses using stainless steel tubes to fabricate all specimens to investigate the flexural behaviour. The parameters were: location of concrete infill stainless steel tube; hollow top and bottom chords; concrete filled upper chord; concrete filled lower chord; concrete filled upper and lower chords. The load carrying capacity, load versus displacement curves, deflections, the failure modes and load-strain curves of all tested specimens were reported. Results showed that the typical failure mode consists of weld fracture and cracks around tubular joints, surface plasticity and upper and lower chord bending. Load capacity, ductility and rigidity of various kinds of trusses differ owing to modifications in the concrete infill place. It is established from the comparison that the truss filled with concrete in upper and lower chords has the highest flexural rigidity and load-carrying capacity, while the truss filled in the upper chord with concrete has the highest ductility. Huang et al. /7/ conducted both experimental tests and numerical analyses. Three CFT truss girders were tested to study the influence of the core concrete strength on the behaviour of CFST truss girders, and numerical analysis to study the influence of parameters like concrete compressive strength, shear proportion of span-to-depth and brace-to-chord strength proportion. Results of experimental tests and FEM analyses showed that the compressive strength of the concrete infill has negligible influence on the CFT truss girders' failure mode.

Machacet et al. /19/ studied numerically the Warren truss with concrete deck slab and determined the longitudinal shear distribution between the concrete and steel, from elastic up to plastic. They proved the nonlinear longitudinal shear distribution is a prerequisite for the design of shear connectors. Han et al. /20/ tested six groups of CFST to estimate the influences of the shear span to depth ratio, the existence of concrete infill, the existence of concrete slab, the angle between chords and diagonal braces, and the dimension of the bottom chord. From the experimental study, the authors indicated that the behaviour and load capacity of CFST trusses are greatly increased in comparison to trusses of hollow steel tube. The ultimate load of the CFST truss with concrete slab is higher than the ultimate load of CFST truss girders and hollow steel tube truss. Hu et al. /21/ studied the flexural behaviour of concrete filled steel tube truss composite (CFSTTC) beams experimentally and analytically. Two CFSTTC beams were tested with different web configurations; one specimen has transverse braces and the other has diagonal and transverse braces. The load capacities, deflection shapes, failure modes, strain responses are evaluated. The specimens' failure mode is different. The failure mode of the specimen with diagonal braces was surface plasticity at the lower chord, and the failure mode of another specimen was surface plasticity at the top chords, local buckling and weld cracks. The specimen with diagonal braces can develop the shear transmute mechanism between upper and lower chords and result in larger load capacity, stiffness, and ductility than the other specimen.

We noted that previous studies on CFST truss girders with concrete deck slab are limited, so this topic needs to be studied extensively. This study offers further investigation on the flexural behaviour of Warren vertical CFST truss girders with reinforced concrete deck slab. The experiments were carried out on eight CFST truss girders. The test parameters are: compressive strength (fcu) of concrete deck slab; compressive strength (fcu) of concrete-filled lower chord; concrete slab existence; location of concrete-filled tube and its existence; the space between shear connectors, and the profile of the lower chord. The deflection, load capacity, failure modes and slip between the concrete slab and steel tube are reported.

EXPERIMENTAL WORK

Eight steel truss girder specimens are designed, as shown in Fig. 1, and tested as part of the experimental program. The truss girders have a 2660 mm length and a 400 mm depth, centre to centre. The top chords are labelled as T, the bottom chords are given the label B. The first and the last vertical braces of all specimens are built up by using steel tubes of 100×100 mm dimensions and 3.8 mm thickness, except the bottom chord of one specimen, installed by using 150×150×4 mm steel tubes and labelled as (BC). The steel tubes of vertical and diagonal braces of dimensions 80 × 80×2.8 mm, for all specimens were welded to chords. The diagonal braces were sloped at 54° from the bottom chord. The distance between vertical braces is 410 mm, centre to centre. The cross-section of the specimens is shown in Fig. 2. Specimens' chords were filled by self-compacting concrete with strength of 50 MPa (labelled as 50), and 30 MPa (labelled as 30). The hollow chords were labelled 0. Reinforced concrete deck slabs, labelled as D, were 2600 mm length, 400 mm width, and 75 mm thickness. These slabs reinforced by ∅8 mm steel bars were merged with the top chord of six trusses by shear channel connectors (U50×25). The distance between shear connector channels was 120 mm

(labelled as S12) for five specimens, and 300 mm (labelled as S30) for one specimen. Table 1 shows the parameters of the test specimens described in this section. Table 2 shows the yield and ultimate stresses of the different steel sections used in the specimens.

Self-compacting concrete (SCC) is adopted in this study to fill the steel tube and casting the deck slabs. Its production needs special materials with a specified production method to meet requirements of the European Federation of National Associations Representing producers and applicators of specialist building products for Concrete (EFNARC) specifications, /22/. SCC contains mineral and chemical admixtures in addition to the conventional materials (cement, sand, gravel and water). The mix proportions of M30, M50 and M60 (Table 3) are adopted for SCC mixes to fill the steel tubes as well as for casting the slabs. The strength of concrete (fcu) is shown in Table 4 for cubic tests and the tests results of the fresh SCC are shown in Table 5.

Table 1. Parameters of the test specimens.

Specimen	fcu (MPa)			S (mm)*
	Deck	Top CFT	Bottom CFT	
D0T50B50	0	50	50	0
D0T50B30	0	50	30	0
D60T50B50S12	60	50	50	120
D30T50B50S12	30	50	50	120
D60T0B50S12	60	0	50	120
D60T0B0S12	60	0	0	120
D60T50B50S30	60	50	50	300
D60T50BC50S12	60	50	50	120

*) S: Distance between shear connectors.

Table 2. Steel properties.

Type of steel section	fy (MPa)	fu (MPa)
Tube (100×100×3.8) mm	328.2	372
Tube (150×150×4) mm	350	421.3
Tube (80×80×2.8) mm	382.9	435.4
Channel (U50×25)	344.4	487
Bar ∅8 mm	401.5	598.8

Table 3. Concrete mixes proportions.*

Mix	Cement	F.A.	C.A.	L.P.	S.P	W/C
M30	300	670	730	110	1%	0.7
M50	450	670	730	90	1.5%	0.42
M60	450	670	730	90	1.75%	0.36

*) F.A. is fine aggregate; C.A. coarse aggregate; L.P. limestone powder; S.P superplasticizer.

Table 4. The results of the cubic sample test.*

Casting Group symbol	Compressive strength (MPa)
CFT30	29.23
CFT50	48.41
D30	31.86
D60	61.47

*) CFT (concrete-filled steel tube); D is concrete block.

Table 5. Results of the fresh concrete test.

Method		Mix symbol			Limitations /22/
		M30	M50	M60	
Slump flow	D (mm)	735	675	790	650 - 800
	T50 (sec)	3.4	3.6	4.5	2 - 5
V-funnel	Tv (sec)	6.7	8.5	9.3	6 - 12
L-Box (BR)		0.89	0.83	0.85	0.8 - 1.0

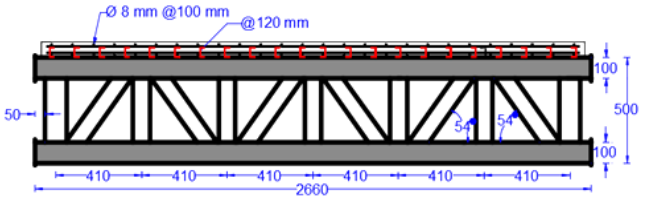

Figure 1. Steel truss girders with deck slab specimens.

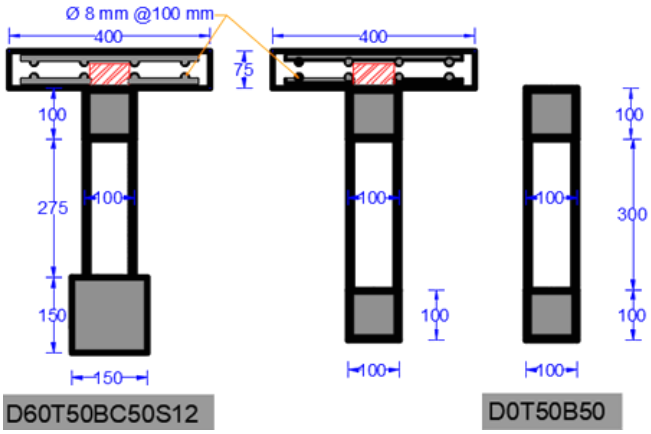

Figure 2. Cross-section of specimens.

Concrete is poured in two stages: the first stage consists of pouring the CFST, then it is left for 10 days to harden the concrete. Then the second stage starts that represents casting of the concrete deck slab.

A hydraulic machine is utilised to test the behaviour of concrete-filled steel tube truss girders with concrete deck slab under concentrated load, placed at the mid-span of the specimens. Girders are placed as simply supported, as well as the lateral support to prevent the specimen from twisting, as shown in Fig. 3.

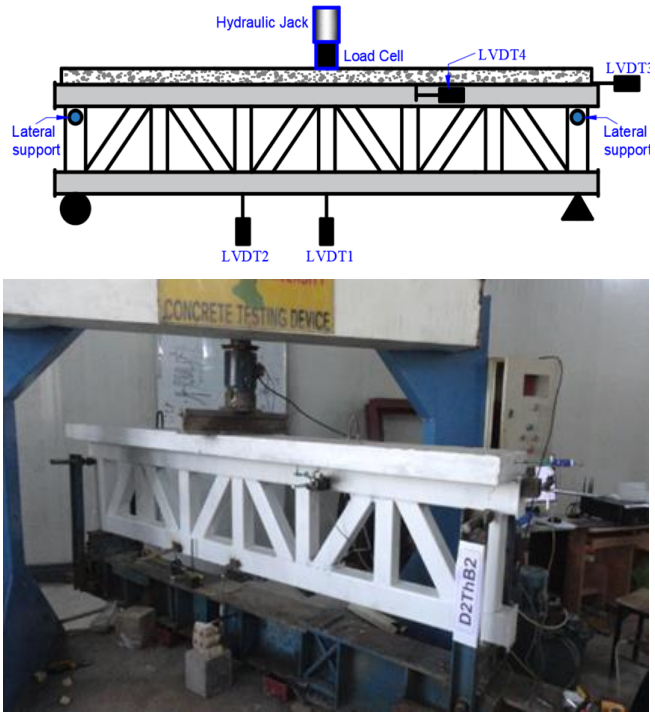

Figure 3. Testing of the specimens.

EXPERIMENTAL RESULTS

In this investigation, two specimens without concrete deck slab and six specimens with concrete deck slab are tested. The test results are arranged in Table 6. The load is recorded at the appearance of first cracks in the concrete deck slab. These eight simply supported CFST truss girders with 2460 mm span are loaded out of the supported plane until failure. Load deflection relationship, failure pattern, deflected shape of the specimens and load-slip relationship for the specimens of the deck slab are recorded and the results are discussed in the following.

Table 6. The load capacity, deflection, load at first crack and the neutral axis of specimens with deck slab.*

Specimen	Pu (kN)	Δ1 (mm)	Δ2 (mm)	P_{cr} (kN)	Ki (kN/mm)	N.A. (mm)
D0T50B50	430.7	30.42	25.50	-	35.1	250
D0T50B30	410.2	23.57	19.85	-	34.6	247.7
D60T50B50S12	525.7	17.18	14.4	361	60.2	384.4
D30T50B50S12	500.0	15.06	12.79	107	56.2	360.2
D60T50BC50S12	613.9	19.09	16.22	447	63.1	346.3
D60T0B50S12	490.6	17.41	14.78	305	46.3	435.7
D60T0B0S12	317.6	13.91	12.28	-	37.3	433.1
D60T50B50S30	535.4	19.41	16.09	256	59.3	384.4

*) Δ1-mid-span deflection; Δ2-third-span deflection; Ki-stiffness; N.A.-neutral axis.

THE FAILURE PATTERN

Two possible failure modes are a characteristic in CFT truss girders: joint shear failure, or the tensile bottom chord fracture. The parametric studies show that if the ratio of brace-to-chord strength is larger than, or equal to 0.8, and the span-to-depth ratio of the shear is larger than, or equal to 4.8, the tensile fracture of the lower chord is the dominant failure mode, but the dominant failure mode is the joint failure mode in the other cases, /14/.

The failure mode is similar for six specimens: D0T50B50 (Fig. 4), D0T50B30 (Fig. 5), D60T50B50S12 (Fig. 6), D30 T50B50S12 (Fig. 7), D60T50BC50S12 (Fig. 8), and D60T 50B50S30 (Fig. 11). It was the joint shear failure (weld fracture), where the proportion of shear span-to-depth was 3.075 for the specimens, in agreement with Huang, /2/.

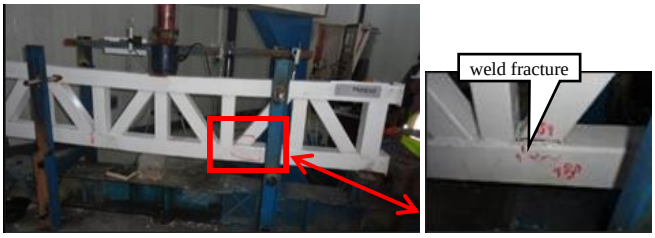

Figure 4. Failure mode of D0T50B50.

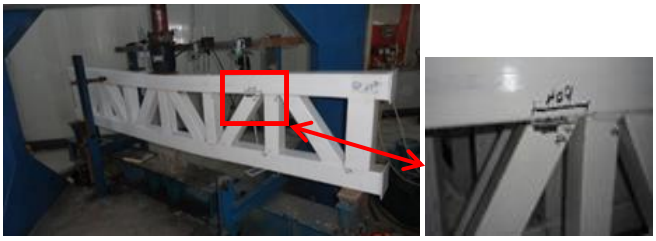

Figure 5. Failure mode of D0T50B30.

Figure 6. Failure mode of D60T50B50S12.

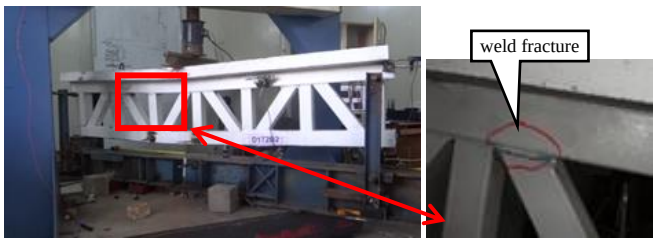

Figure 7. Failure mode of D30T50B50S12.

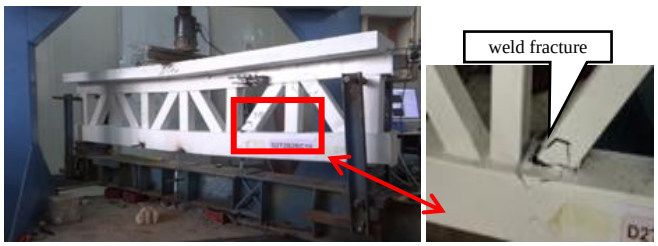

Figure 8. Failure mode of D60T50BC50S12.

The failure mode of D50T0B50S12 is surface plasticity failure, as shown in Fig. 9. This is because the top chord is hollow. The failure mode of D50T0B0S12 is plasticity failure, as shown in Fig. 10, because the bottom chord is hollow.

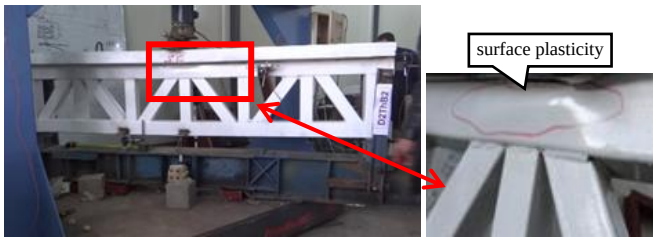

Figure 9. Failure mode of D60T0B50S12.

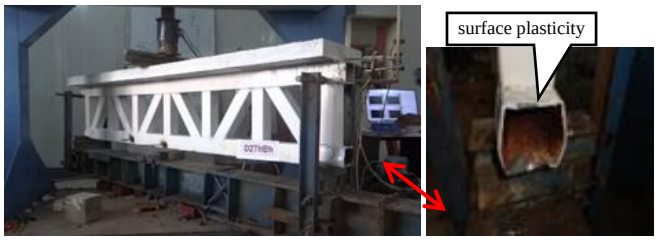

Figure 10. Failure mode of D60T0B0S12.

Figure 11. Failure mode of D60T50B50S30.

CRACKS OF CONCRETE SLAB

The neutral axis is calculated for all specimens as shown in Table 6 by the classical method. The concrete slab is in compression for all specimens before applying the load. The neutral axis moves upwards when increasing the load during the test because of expansion in the tension zone. The load is recorded at the appearance of cracks in concrete deck slab as shown in Table 6. The crack load is 361 kN for specimen D60T50B50S12. This means that the neutral axis of D60T50B50S12 is moved upward by 115 mm at this load, as shown in Fig. 2. While for specimen D60T50BC50 S12, the crack load is 447 kN and the neutral axis moves upwards by 178 mm at this load, meaning that it is higher by 23.82 % than in specimen D50T50B50S12. The reason of the delay in the appearance of concrete slab cracks in D50T50BC50S12 is that the neutral axis of this specimen is lower than the neutral axis in specimen D60T50B50S12. Table 6 shows that cracks in specimen D60T0B50S12 began less than in specimen D50T50B50S12 by 15.51 %. The reason is the surface plasticity failure in the top chord, caused by an increase in bending of the concrete slab, resulting in the rising of the neutral axis upward. The cracks in specimen D50T0B0S12 are not obtained. Because of the limited curvature of the concrete slab, the surface plasticity failure at the supports leads to the decline of the whole model. The load when cracks appeared in D60T50B50S30 was less by 29.1 % than in specimen D50T50B50S12. This attributed to the interaction that reduced the concrete slab restriction, and this allowed the concrete to slip horizontally more than in the other specimens. The crack appeared early in the concrete slab of specimen D30T50B50S12, at load 107 kN, because the strength of the concrete slab is lower than in the other specimens.

DEFLECTION OF SPECIMENS

Deflections are gauged at the mid-, third- and quarter-span for every loading increment for two specimens without deck slab. The deflections were gauged also at mid-span and third-span for every loading increment, for six specimens of the deck slab. From load-deflection curves, it can be noted that the relationship is approximately linear until yield load, then it becomes nonlinear, i.e. inelastic deformation continues and the slope of the load-deflection relationship of the specimen begins to increase until failure. When comparing the stiffness values of the specimens, we found that the lowest value of the stiffness is in specimen D0T50B30, and the highest value is for specimen D60T50B C50S12, as shown in Table 7.

Figure 12 shows deflection shapes for specimens 0.25Pu, 0.5Pu, 0.75Pu, 0.9Pu and Pu.

Table 7. Ultimate load and slip at end-slab and third-span.

Specimen	Pu (kN)	End-slip (mm)	Third-span slip (mm)
D60T50B50S12	525.65	0.0616	0.3581
D30T50B50S12	500.07	0.0717	0.2283
D60T50BC50S12	613.92	-0.0429	0.2590
D60T0B50S12	490.60	0.1051	0.1870
D60T0B0S12	317.64	0.0334	0.1058
D60T50B50S30	535.39	0.6603	1.4571

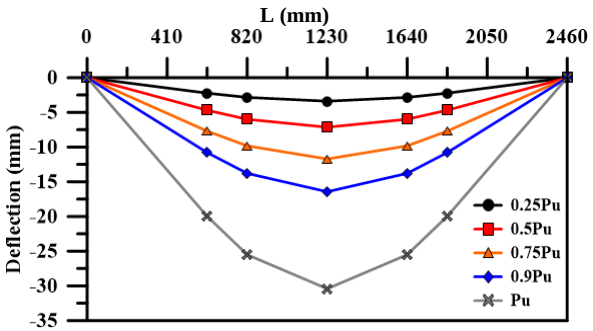

a) D0T50B50

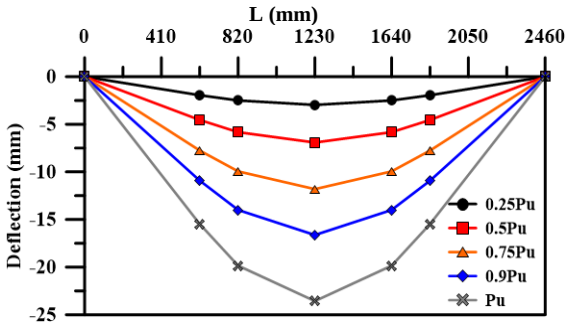

b) D0T50B30

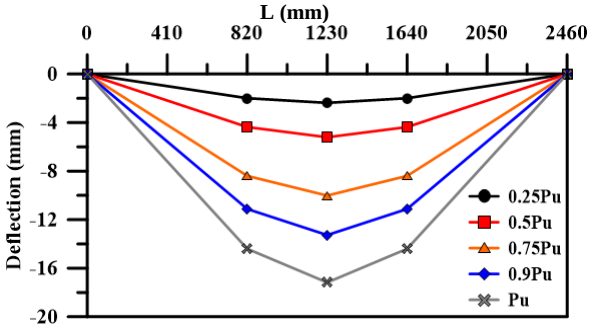

c) D60T50B50S12

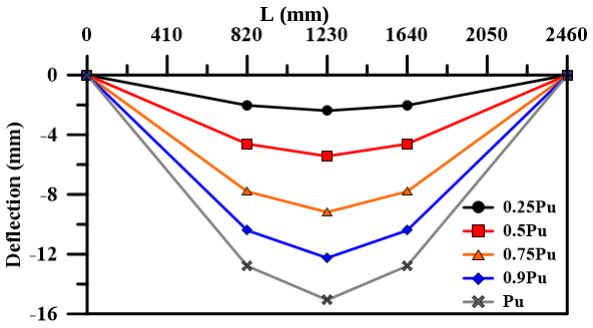

d) D30T50B50S12

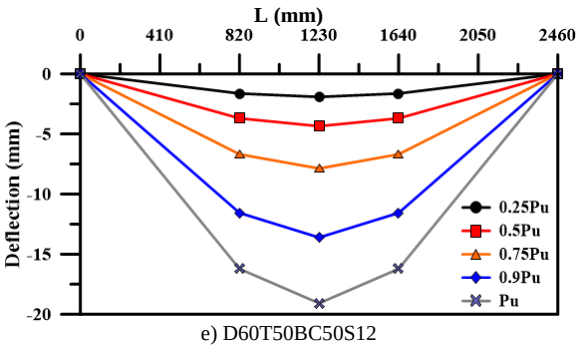

e) D60T50BC50S12

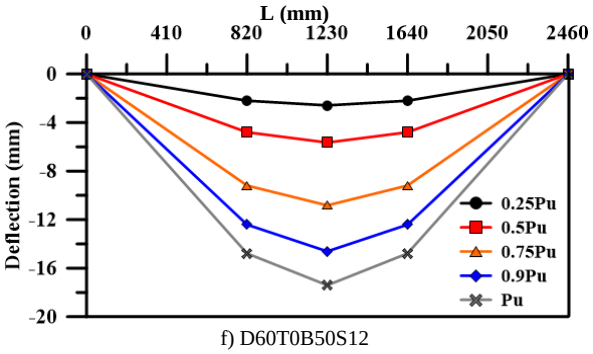

f) D60T0B50S12

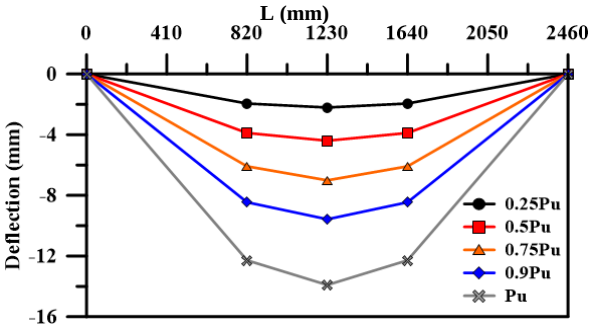

g) D60T0B0S12

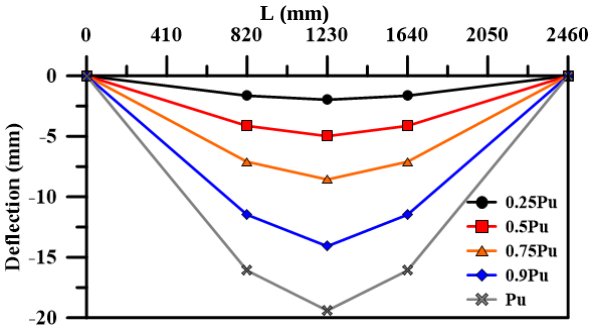

h) D60T50B50S30

Figure 12. Deflected shape of specimens.

Effect of the strength of concrete-filled bottom chord

Figure 13 shows that the load capacity of D0T50B50 is higher than for D0T50B30 by 4.76 % due to increasing the strength of CFST in the bottom chord, and is identical to Huang /7/, where he proved that increasing the strength of concrete used to fill the bottom chord leads to increased loading capacity. Figure 13 shows the load-deflection relationship at mid-span of the two specimens: D0T50B50 and D0T50B30. Figures 14 and 15 show the load-deflection relationship of D0T50B50 and D0T50B30, respectively at the mid-, third-, and quarter-span.

Effect of the strength of concrete deck slab

When comparing the influence of the concrete slab in specimens D60T50B50S12 and D30T50B50S12 with specimen D0T50B50 without slab, that have the same steel section of the chords and the strength of concrete inside the chords, as shown in Table 7, it can be noted that the ultimate load of the specimens D60T50B50S12 and D30T50B50S12 is higher than that of specimen D0T50B50 by 22.05 % and 16.1 %, and the deflection at mid-span is less by 43.52 % and 50.5 %, respectively. This behaviour is due to from the deck slab and the top chord that were exposed to compres

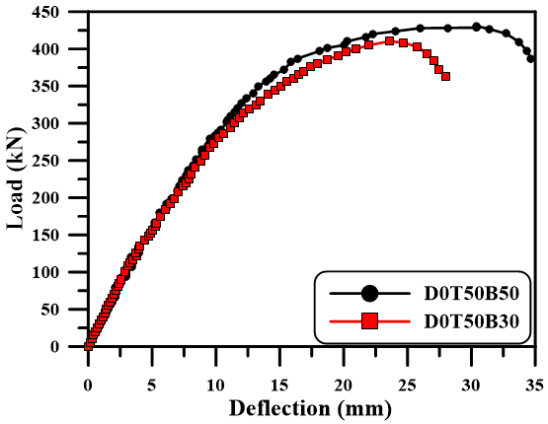

Figure 13. Load-deflection relationship of D0T50B50 and D0T50B30 at mid-span.

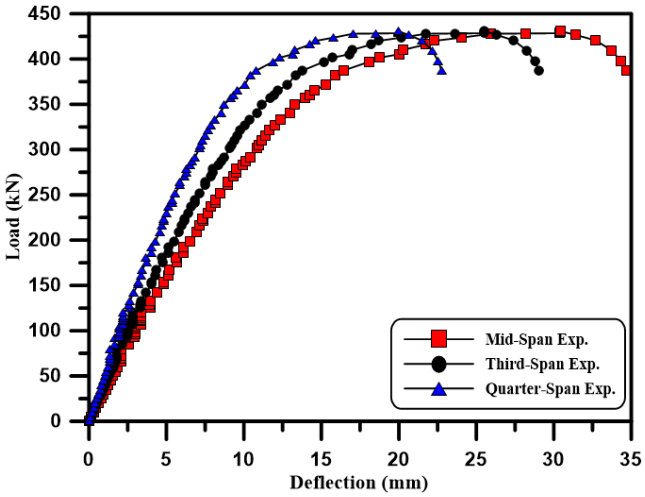

Figure 14. Load-deflection of D0T50B50.

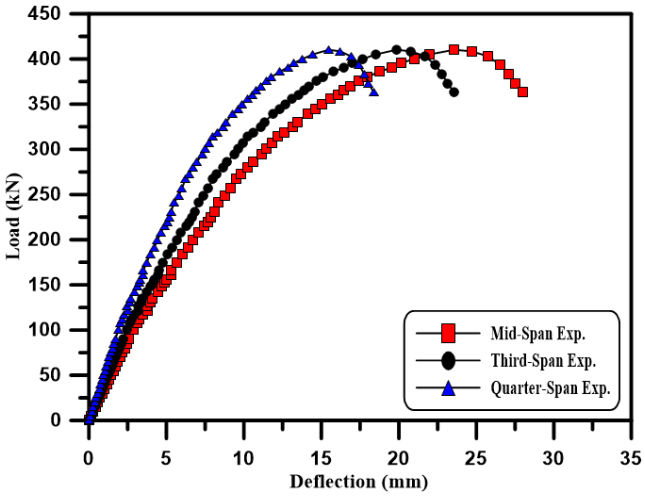

Figure 15. Load-deflection of D0T50B30.

sive stress during loading. The existence of concrete deck slab increases the compressive resistance of the specimen (Fig. 16). Figures 14, 17 and 18 show the load-deflection relationship of D0T50B50, D60T50B50S12 and D30T50B5 0S12, respectively.

Effect of concrete filled chords

Specimens D60T0B50S12 of hollow top chord and D60T0B0S12 of two hollow chords (top and bottom) with

specimen D60T50B50S12 share the same steel tube section in the chords and the same strength of the concrete deck slab. Table 7, and Fig. 19 show that the ultimate load of D60T0B50S12 and D60T0B0S12 is less than for D60T50B 50S12 by 6.67 % and 39.57 %, respectively, and the deflection at mid-span of D60T0B50S12 is higher than that of D60T50B50S12 by 1.3 %. The deflection at mid-span of D60ThBhS12 is less than that of D60T50B50S12 by 19 %. Load-deflection relationship of D60T0B50S12 and D60T0 B0S12 at mid- and third-span is shown in Figs. 20 and 21,

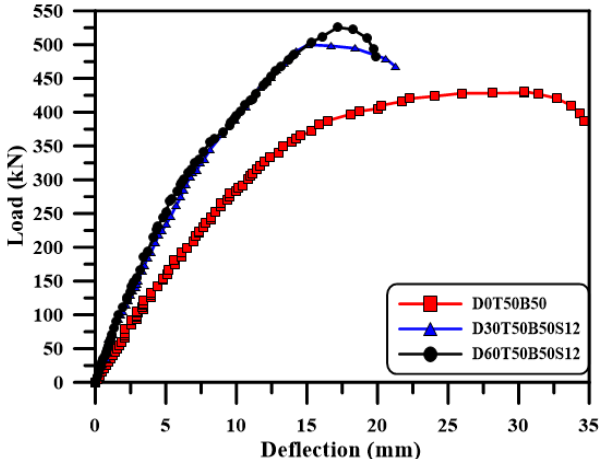

Figure 16. Load-deflection relationship of D0T50B50, D60T50B50S12 and D30T50B50S12 at mid-span.

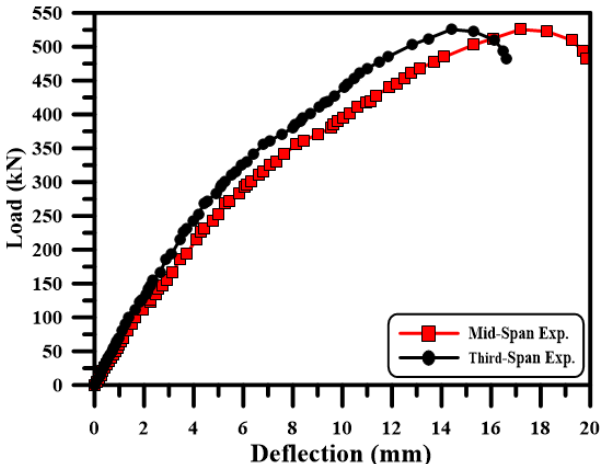

Figure 17. Load-deflection of D60T50B50S12 .

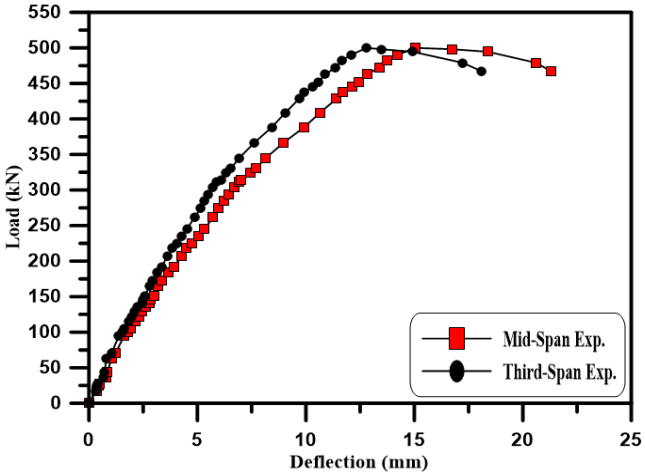

Figure 18. Load-deflection of D30T50B50S12.

respectively. The reason for these results is that the hollow top chord of specimen D60T0B50S12 reduced the stiffness (46.25 kN/mm) in the compression zone. This leads to the reduction of ultimate load of the specimen. Also, the hollow top and bottom chords of D60T0B0S12 reduced the stiffness (37.28 kN/mm) and the ultimate load of the specimen. The compression and tension resistances increase when the tube is filled with concrete and this prevented the buckling inward to the top chord, and restrained the pinching to the bottom chord, /7/. In tensile strength, the CFST has a higher value than that of the hollow tube, /8/.

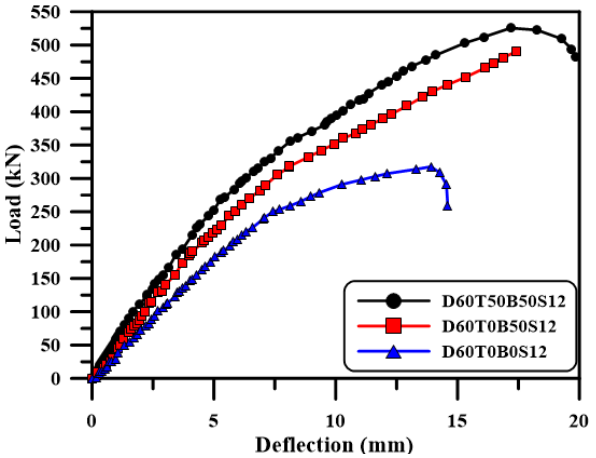

Figure 19. Load-deflection relationship of D60T50B50S12, D60T0B50S12 and D60T0B0S12 at mid-span.

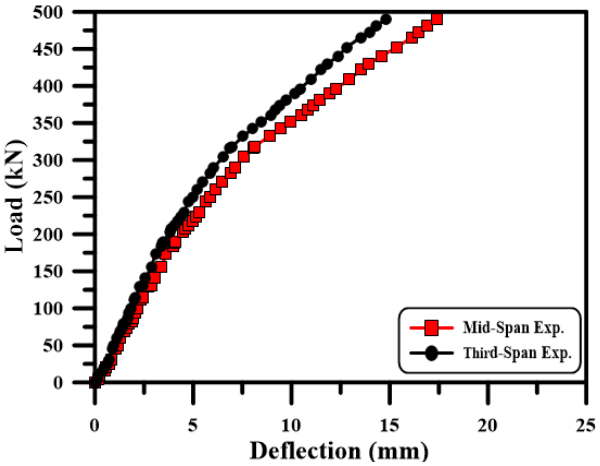

Figure 20. Load-deflection of D60T0B50S12.

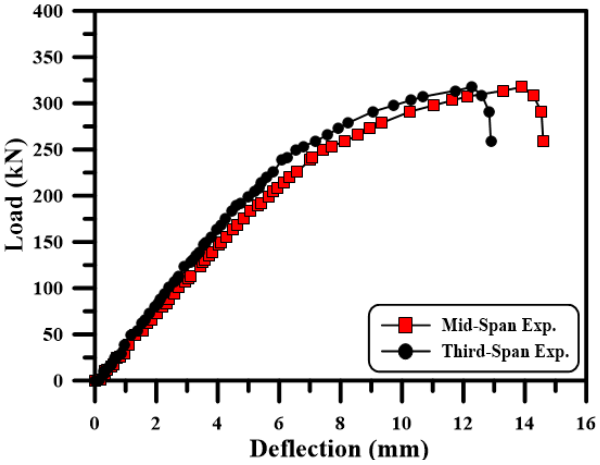

Figure 21. Load-deflection of D60T0B0S12.

Effect of bottom chord dimensions

Table 7 and Fig. 22 show that the ultimate load of specimen D60T50BC50S12 of the bottom chord dimensions of 150×150 mm is higher by 16.79 %. The deflection also at mid-span is higher by 11.12 %, compared to that of specimen D60T50B50S12. The reason for these results is that the largest section of the bottom chord in specimen D60T50 BC50S12, located at the tension zone, made it more ductile and more tensile resistant, due to higher loading capacity. Figure 23 shows the mid- and third-span load-deflection relationship in specimen D60T50BC50S12.

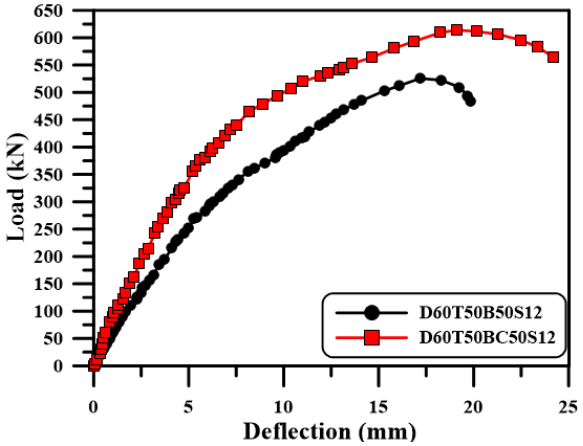

Figure 22. Load-deflection relationship of D60T50B50S12 and D60T50BC50S12 at mid-span.

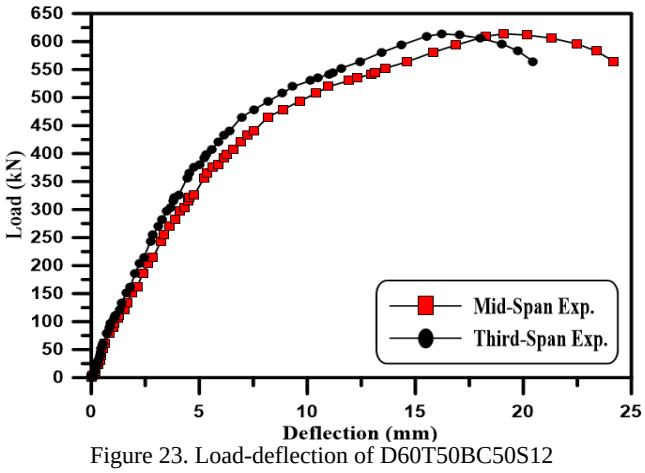

Figure 23. Load-deflection of D60T50BC50S12

Effect of spacing between shear connectors channel

Two spacings of shear connectors, 150 and 300 mm are used to study its influence on the behaviour of CFST girders with deck slab. Results of ultimate load have a slight difference. The mid-span deflection of D50T50B50S30 is greater by 13 %, than that in specimen D50T50B50S12. The ultimate load and difference of the deflection are shown in Table 7 and in Fig. 24. Figure 25 shows the load-deflection relationship at mid- and third-span of specimen D50T50B5 0S30.

HORIZONTAL SLIP

In interfacial complications, forces are transmitted by normal and tangential (shear) stresses from the body to another /23/. The slip is the horizontal difference between the concrete slab and the steel tube, resulting from their movement, due to the horizontal shear force during loading.

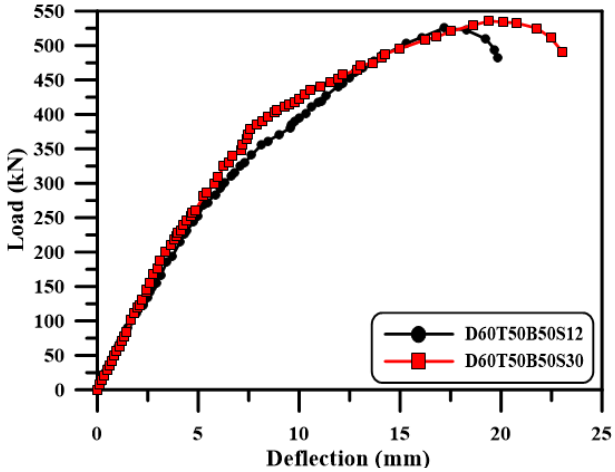

Figure 24. Load-deflection relationship of D50T50B50S12 and D50T50B50S30 at mid-span.

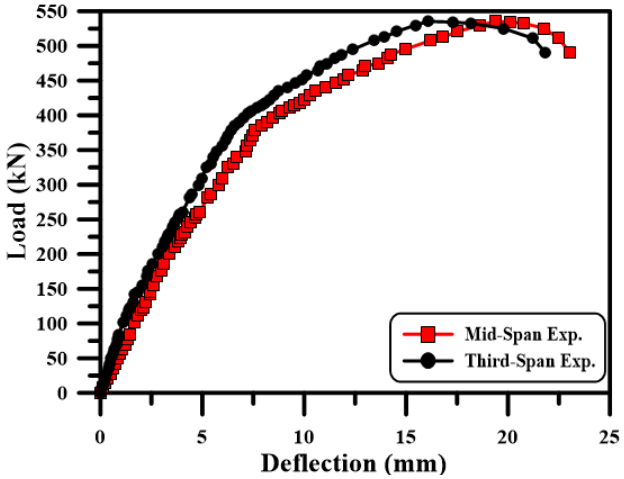

Figure 25. Load-deflection of D60T50B50S30.

Table 7 shows that the total slip at the end of D60T50B 50S12 (Fig. 26) is less by 41.39 % than the slip of D60T0 B50S12 (Fig. 29), because of the bending at the concrete slab due to the plasticity failure of the hollow upper chord in specimen D60T0B50S12. The slip of D60T0B0S12 (Fig. 30) is less by 45.78 % than in D60T50B50S12, because of the plasticity failure at the bottom chord, which leads to the decent of the whole specimen and reduces the bending at the upper chord and concrete slab.

The slip of specimen D60T50B50S30 (Fig. 31) is higher than the rest of the specimens, because the distance between shear connectors is greater than in other specimens. The slip of D30T50B50S12 (Fig. 27) is higher by about 16.4 % than the slip of D60T50B50S12, because the strength of the concrete slab in D30T50B50S12 is less than the strength of the concrete slab in D60T50B50S12, although the ultimate load is lower.

The slip of specimen D60T50B50S30 (Fig. 31) is higher than the rest of the specimens, because the distance between shear connectors is greater than in other specimens. The slip of D60T50BC50S12 differs in behaviour from other specimens. Figure 28 shows that the slip at the end of the slab is opposing the slip for the rest of the specimens.

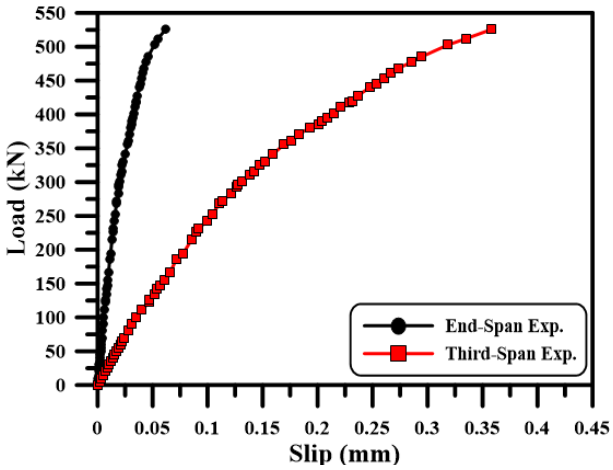

Figure 26. Load-slip of D60T50B50S12.

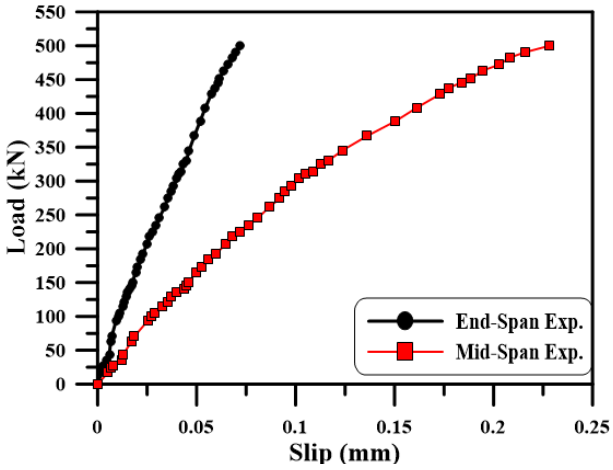

Figure 27. Load-slip of D30T50B50S12.

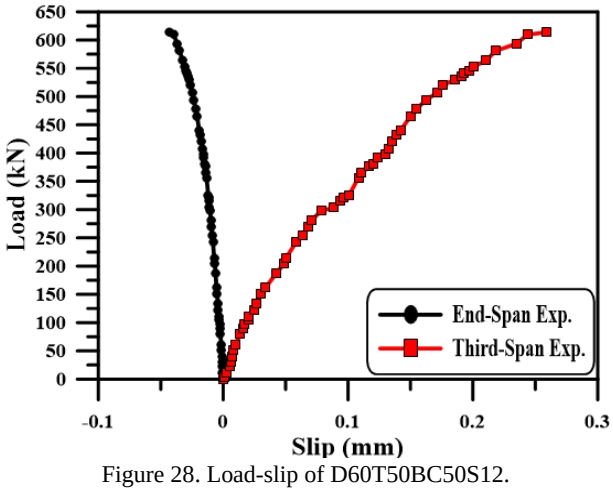

Figure 28. Load-slip of D60T50BC50S12.

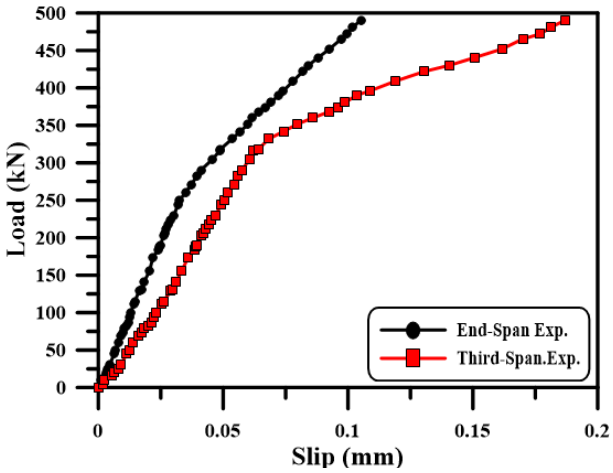

Figure 29. Load-slip of D60T0B50S12.

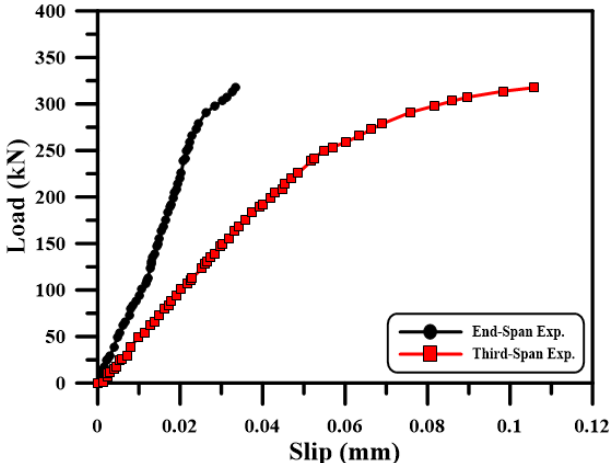

Figure 30. Load-slip of D60T0B0S12.

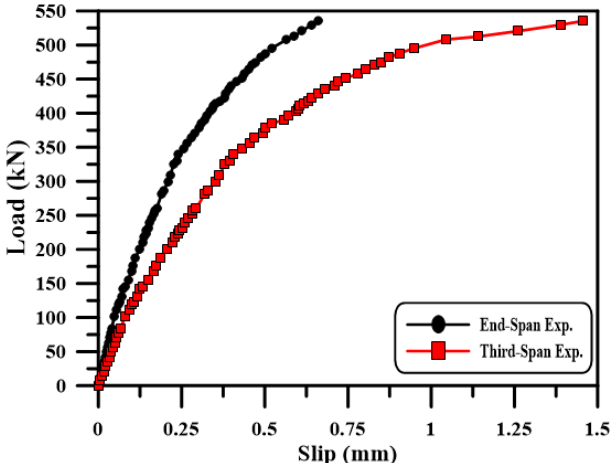

Figure 31. Load-slip of D60T50B50S30.

CONCLUSIONS

In this study, the experimental tests are adopted to analyse the behaviour of Warren-vertical CFT truss girders with concrete deck slab under concentrated load at the mid-span. Experimental tests on two specimens without deck slab and six specimens with deck slab are performed. From this study, the following conclusions can be reported:

- The load capacity of the CFST truss with deck slab is higher and the deflection is less than for the CFST truss without deck slab. The load capacity of the strength of concrete slab (60 MPa and 30 MPa) is higher by 22.05% and 16.1% and the deflection at mid-span is less by 43.52% and 50.5% respectively, than that of the specimen without concrete deck slab.
- The strength of concrete slab effects the ultimate load and the slip between the concrete slab and steel tube. When the strength of concrete slab is reduced from 60 MPa to 30 MPa, the ultimate load decreases by 4.87 % and the slip decreases by 12.34 %. This has also caused the appearance of early cracks.

- The increase in steel dimensions of the bottom chord form 100×100×3.8 mm to 150×150×4 mm increased the ultimate load by 16.79% and the deflection at mid-span by 11.12 %, and caused delay in the appearance of cracks in the concrete slab.
- Steel tubes of upper chord filled by concrete prevent surface plasticity failure of the upper chord under loading and increase the ultimate load by 6.67 %. Also, filled lower chord with concrete prevents surface plasticity failure above the supports and results in increasing the ultimate load by 39.57 %.
- Increasing the distances between the shear connectors has a slight effect on the ultimate load, as well as increasing the slip between the concrete slab and the steel tube by 972 %.
- Increasing the strength of concrete, used to fill the bottom chord, from 30 to 50 MPa leads to an increase in the loading capacity by 5 %.

REFERENCES

1. Nie, J., Fan, J., Cai, C.S. (2008), *Experimental study of partially shear-connected composite beams with profiled sheeting*, Eng. Struct. 30(1): 1-12. doi: 10.1016/j.engstruct.2007.02.016
2. Nakamura, S.-I. (2002), *Bending behavior of composite girders with cold formed steel U section*, J Struct. Eng. (ASCE). 128(9): 1169-1176. doi: 10.1061/(asce)0733-9445(2002)128:9(1169)
3. Han, L.-H., Li, W., Bjorhovde, R. (2014), *Developments and advanced applications of concrete-filled steel tubular (CFST) structures: Members*, J Construct. Steel Res. 100: 211-228. doi: 10.1016/j.jcsr.2014.04.016
4. Chen, Y., Feng, R., Wang, L. (2017), *Flexural behaviour of concrete-filled stainless steel SHS and RHS tubes*, Engineering Structures, 134(C): 159-171. doi: 10.1016/j.engstruct.2016.12.03
5. Chen, Y., Wang, K., Feng, R., et al. (2017), *Flexural behaviour of concrete-filled stainless steel CHS subjected to static loading*, J Construct. Steel Res. 139: 30-43. doi: 10.1016/j.jcsr.2017.09.009
6. Shallal, M.A. (2018), *Flexural behavior of concrete-filled steel tubular beam*, in 2018 International Conference on Advance of Sustainable Engineering and its Application (ICASEA), 2018, IEEE. doi: 10.1109/ICASEA.2018.8370974
7. Huang, W., Lai, Z.-C., Chen, B., et al. (2018), *Concrete-filled steel tube (CFT) truss girders: Experimental tests, analysis, and design*, Eng. Struct. 156: 118-129. doi: 10.1016/j.engstruct.2017.11.026
8. Han, L.-H., He, S.-H., Liao, F.-Y. (2011), *Performance and calculations of concrete filled steel tubes (CFST) under axial tension*, J Construct. Steel Res. 67(11): 1699-1709. doi: 10.1016/j.jcsr.2011.04.005
9. Lai, Z., Varma, A.H. (2015), *Noncompact and slender circular CFT members: Experimental database, analysis, and design*, J Construct. Steel Res. 106: 220-233. doi: 10.1016/j.jcsr.2014.11.005
10. Lai, Z., Varma, A.H., Griffis, L.G. (2015), *Analysis and design of noncompact and slender CFT beam-columns*, J Struct. Eng. 142(1): 04015097. doi: 10.1061/(ASCE)ST.1943-541X.0001349
11. Lai, Z., Varma, A.H., Zhang, K. (2014), *Noncompact and slender rectangular CFT members: Experimental database, analysis, and design*, J Construct. Steel Res. 101: 455-468. doi: 10.1016/j.jcsr.2014.06.004
12. Chan, S.L., Fong, M. (2011), *Experimental and analytical investigations of steel and composite trusses*, Advanced Steel Constr. 7(1): 17-26. doi: 10.18057/IJASC.2011.7.1.2
13. Huang, W., Fenu, L., Chen, B., et al. (2012), *Resistance of welded joints of concrete-filled steel tubular truss girders*, 10th Int. Conf. on Advances in Steel Concrete Composite and Hybrid Structures, 2012: 547-554. doi: 10.3850/978-981-07-2615-7_067
14. Xu, W., Han, L.-H., Tao, Z. (2014), *Flexural behaviour of curved concrete filled steel tubular trusses*, J Construct. Steel Res. 93: 119-134. doi: 10.1016/j.jcsr.2013.10.015
15. Chen, Y., Feng, R., Gao, S. (2015), Experimental study of concrete-filled multiplanar circular hollow section tubular trusses, Thin-Walled Struct. 94: 199-213. doi: 10.1016/j.tws.2015.04.013
16. Fu, Z.-Q., Ji, B.-H., Zhu, W., Ge, H. (2016), *Bending behaviour of lightweight aggregate concrete-filled steel tube spatial truss beam*, J Central South Univ. 23(8): 2110-2117. doi: 10.1007/s11771-016-3267-x
17. Huang, Y.-H., Liu, A.-R., Fu, J.-Y., Pi, Y.-L. (2017), *Experimental investigation of the flexural behavior of CFST trusses with interfacial imperfection*, J Construct. Steel Res. 137: 52-65. doi: 10.1016/j.jcsr.2017.06.009
    Zhou, W., Chen, Y., Wang, K., et al. (2017), *Experimental research on circular concrete filled stainless steel tubular truss*, Thin-Walled Struct. 117: 224-238. doi: 10.1016/j.tws.2017.04.026
18. Machacek, J., Cudejko, M. (2011), *Composite steel and concrete bridge trusses*, Eng. Struct. 33(12): 3136-3142. doi: 10.1016/j.engstruct.2011.08.017
19. Han, L.-H., Xu, W., He, S.-H., Tao, Z. (2015), *Flexural behaviour of concrete filled steel tubular (CFST) chord to hollow tubular brace truss: experiments*, J Construct. Steel Res. 109: 137-151. doi: 10.1016/j.jcsr.2015.03.002
20. Hu, B., Wang, J. (2017), *Experimental investigation and analysis on flexural behavior of CFSTTC beams*, Thin-Walled Struct. 116: 277-290. doi: 10.1016/j.tws.2017.03.024
21. BIBM, Cembureau, ERMCO, EFCA, EFNARC (2005), The European Guidelines for Self-Compacting Concrete. Specification, Production and Use. http://www.efnarc.org/pdf/SCCGuidelinesMay2005.pdf
22. Brown, C.J., Darwin, D., McCabe, S.L. (1993), *Finite element fracture analysis of steel-concrete bond*, SM Report 36, University of Kansas Center for Research, Inc., p.98.